

**December 10, 2018**

SunPower Corporation

77 Rio Robles

San Jose, CA 95134

**Re: SunPower Response to InClimate Solutions Request for Comments on Illinois Adjustable Block Program Draft Guidebook**

**Introduction**

As one of the world's most innovative and sustainable energy companies, SunPower (NASDAQ:SPWR) provides a diverse group of customers with complete solar solutions and services. Residential customers, businesses, governments, schools and utilities around the globe rely on SunPower's more than 30 years of proven experience. From the first flip of the switch, SunPower delivers maximum value and superb performance throughout the long life of every solar system. SunPower is currently the No. 1 commercial solar provider in America with the most megawatts installed and the top residential solar manufacturer according to Wood Mackenzie (formerly GTM Research), with a footprint around the world. We design, manufacture and install the world's highest efficiency solar technology. Based in Silicon Valley and founded over 30 years ago, SunPower has deployed more than 9.2GW solar PV globally.

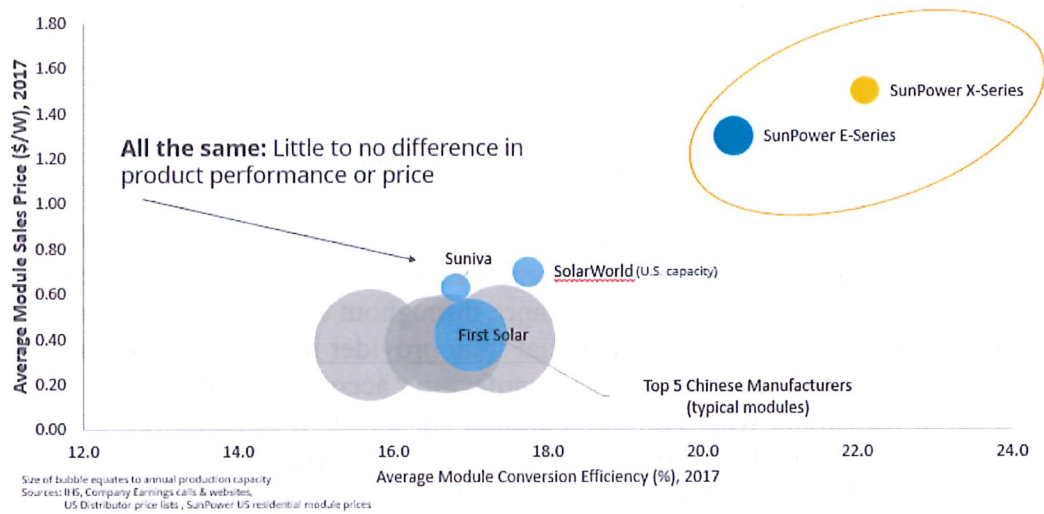
SunPower applauds the Illinois Power Agency and the Program Administrator, InClimate Solutions, for the work they have put in developing this program. On November 28, 2018, the Illinois Power Agency released the Illinois Adjustable Block Program Draft Guidebook and requested additional written feedback from stakeholders. We respectfully submit the following comments in order to ensure a fair process and REC payments that accurately reflect the 15-year solar production output.

**SunPower Performance and Degradation Rate**

Section 4- REC Quantity Calculation (page 15 of 33) mentions that "The application portal will automatically calculate the PVWatts estimated production and the standard capacity factors of 16.42% for fixed mount or single axis trackers and 19.32% for dual axis tracking systems." We are concerned that a default capacity factor for all projects may encourage the use of sub-standard, lower quality products. SunPower products have a long third-party verified history of high performance and we think that they should receive the appropriate quantity of RECs for

producing higher value. This can be achieved by allowing us to calculate RECs based on a higher Capacity Factor when justified by the systems expected production given superior technology

SunPower technology is fundamentally different, and better. IBC products are highly differentiated as shown in the graph below. SunPower possesses a record breaking 24.1% silicon solar panel efficiency, measured by the National Renewable Energy Laboratory (NREL). More technical details about the SunPower products are included in the *attached slide deck, which also includes confidential information, so we kindly ask IPA and InClima Solutions not to publish it along with the SunPower comments.*



For these reasons, the Office of the U.S. Trade Representative has filed with the Federal Register office, for publication on Sept. 19, 2018, a decision that certain interdigitated back contact (IBC) solar cells and modules, within specific size and power ranges, will be excluded from the solar tariffs imposed in January pursuant to Section 201 of the Trade Act. As a result, SunPower’s IBC cells and modules are excluded from Section 201 import tariffs. This proves the superior technology of SunPower products.

Earlier this year, in partnership with the National Renewable Energy Laboratory (NREL), the U.S. Department of Energy's primary national laboratory for renewable energy and energy efficiency research and development, SunPower developed a robust method to calculate solar panel degradation which is something all solar panels experience, but at varying rates (also attached). When this method was applied to eight years of energy performance data from 264 SunPower solar systems operating at various locations worldwide, it proved that SunPower panels degrade at a median rate of 0.2 percent per year: 70 percent less than the annual degradation rate for Conventional Panels.

SunPower backs its performance by proving the lowest degradation for performance and power warranty to our customers. For instance, our E series panels come with a warranty that “the

power of PV modules will be at least 98% of the minimum peak power rating for the first year, and will decline by no more than 0.25% per year for the following 24 years.” As a result, SunPower believes that the 0.5% per year average output degradation factor that the Long-Term Renewable Resources Procurement Plan is using is not reflective of the performance of SunPower products.

## Energy Modeling Tools

The same section of the Draft Guidebook also mentions that “Any proposed alternate capacity factor that is calculated using a proprietary third-party software tool will require the Approved Vendor to provide a copy of the third-party software tool with appropriate licenses to the Program Administrator as well as providing all inputs to the tool in a manner which will allow the Program Administrator to replicate the generation claimed. The Program Administrator will accept alternate capacity factors on a case by case basis after reviewing the methodology used to determine such alternate capacity factor.” This is an important consideration for modeling SunPower high-efficiency technologies, as PVWatts does not distinguish between the performance characteristics of different PV technologies.

In fact, PVWatts in their [website](#) provides that following disclaimer (under Help – see the screen shot below), which clearly indicates that PVWatts is a “quick and dirty” approach and not accurate for final system production calculation.

**Important Note.** PVWatts<sup>®</sup> is suitable for very preliminary studies of a photovoltaic system that uses modules (panels) with crystalline silicon or thin film photovoltaic cells. PVWatts<sup>®</sup> production estimates do not account for many factors that are important in the design of a photovoltaic system. If you are using PVWatts<sup>®</sup> to help design a system, you should work with a qualified professional to make final design decisions based on an assessment of the system location and using more detailed engineering design and financial analysis tools.

SunPower is using PVSIM, which is an online, publicly-available energy modelling tool developed internally, updated by industry experts and validated by in-house and 3rd-party testing. It is the highest-accuracy simulation tool available, for all modules but especially SunPower ones. SunPower uses measured data from our 600+ fielded systems to validate our model accuracy. Finally, it is an open tool that everyone can use.

PVSIM has been proven by 3<sup>rd</sup> party engineers. It has been audited by BEW/DNV Engineering, an independent engineering firm (full report attached - please keep confidential):

“BEW using PVSIM obtained results closer to measurements than BEW using PVSyst with comparable modeling assumptions.”

“PVSIM generally uses state-of-the-art algorithms that should yield accurate results.”

“BEW agrees that PVSIM is able to simulate portfolios of actual installed systems to within 1%+/-2.3%.”

“SAM/PVWatts is a relatively crude simulator, and the observed departure from measured performance is excessive.”

Finally, SunPower has installed a 10 MW (DC) solar system in Cook County, IL for Exelon Energy, which remains one of the largest urban solar installations in the country. Since 01/2014, SunPower modules have produced 100% of the PV production modelled in PVSIm.

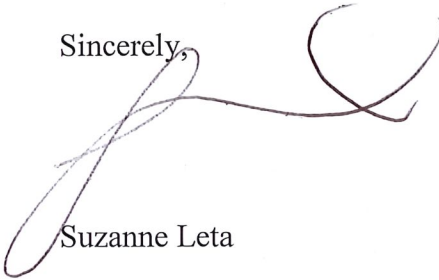
SunPower is happy to provide login credentials (included in the confidential slide deck) and a training session to the Program Administrator as well as the inputs for any project we submit, so InClima can confirm the annual generation that SunPower submits in its applications.

### **Conclusion**

For all the above mentioned reasons, we urge the Program Administrator to allow SunPower to (1) submit 15-year production estimates using PVSIm, (2) extend the lower degradation rate that has been demonstrate for our technologies, and (3) use the capacity factors as calculated by PVSIm. As an alternative, we suggest that bidders be allowed to submit a greater capacity factor at the time of the bid, with production certified by a licensed Illinois engineer at the time of PTO. If the certification is not provided at PTO, the standard factors would be applied at that time.

SunPower appreciates the opportunity to respectfully submit these comments. Thank you for considering them.

Sincerely,

A handwritten signature in dark ink, appearing to read 'Suzanne Leta', with a large, stylized flourish extending to the right.

Suzanne Leta

Global Market Strategy

### **Attachments**

1. Copy of the Federal Register document which explains the exclusion.
2. Slide deck: Solar Technology & Performance for Illinois (please note that this is confidential)
3. 3<sup>rd</sup> party PVSIm Evaluation report: BEW engineers (to remain confidential)
4. NREL paper on Robust PV Degradation Methodology and Application



Billing Code 3290-F8

**OFFICE OF THE UNITED STATES TRADE REPRESENTATIVE**

**[Docket Number USTR-2018-0001]**

**Exclusion of Particular Products From the Solar Products Safeguard Measure**

**AGENCY:** Office of the United States Trade Representative.

**ACTION:** Notice.

**SUMMARY:** Pursuant to authority provided by the President, the U.S. Trade Representative (Trade Representative) has determined that particular products should be excluded from the safeguard measure applied to certain solar products and is modifying subchapter III of chapter 99 of the Harmonized Tariff Schedule of the United States (HTS) as set forth in the Annex of this notice to implement these exclusions.

**DATES:** The modifications to the HTS set forth in the Annex are applicable with respect to articles entered, or withdrawn from a warehouse for consumption, on or after 12:01 am EST, on **[INSERT DATE OF PUBLICATION IN THE FEDERAL REGISTER]**.

**FOR FURTHER INFORMATION CONTACT:** Victor Mroczka, Office of WTO and Multilateral Affairs, at [vmroczka@ustr.eop.gov](mailto:vmroczka@ustr.eop.gov) or (202) 395-9450, or Dax Terrill, Office of General Counsel, at [Dax.Terrill@ustr.eop.gov](mailto:Dax.Terrill@ustr.eop.gov) or (202) 395-4739.

**SUPPLEMENTARY INFORMATION:**

**I. Background**

On November 13, 2017, the U.S. International Trade Commission (ITC) submitted a report to the President under section 201 of the Trade Act of 1974, as amended (19 U.S.C. 2251), finding that crystalline silicon photovoltaic (CSPV) cells and other CSPV products containing these cells are being imported into the United States in

such increased quantities as to be a substantial cause of serious injury to the domestic industry producing an article that is like or directly competitive with the imported products. The scope of this investigation did not cover:

- Thin film photovoltaic products produced from amorphous silicon (a-Si), cadmium telluride (CdTe), or copper indium gallium selenide (CIGS).

- CSPV cells, not exceeding 10,000 mm<sup>2</sup> in surface area, that are permanently integrated into a consumer good whose primary function is other than power generation and that consumes the electricity generated by the integrated CSPV cell.

Where more than one CSPV cell is permanently integrated into a consumer good, the surface area for purposes of this exclusion is the total combined surface area of all CSPV cells that are integrated into the consumer good.

- CSPV cells, whether or not partially or fully assembled into other products, if such CSPV cells were manufactured in the United States.

The President, taking into consideration the separate recommendations of the ITC Commissioners on remedy and the recommendation of the Trade Policy Staff Committee, determined to take action and issued Proclamation 9693 on January 23, 2018, to impose a safeguard measure with respect to the imported CSPV products. The President determined to implement the safeguard measure as: (1) a tariff-rate quota on imports of CSPV cells not partially or fully assembled into other products, imposed for a period of 4 years, with unchanging within-quota quantities and annual reductions in the rates of duty applicable to goods entered in excess of those quantities in the second, third, and fourth years, as provided in Annex I to the proclamation; and (2) an increase in duties on imports of CSPV products containing these cells, imposed for a period of 4 years, with

annual reductions in the rates of duty in the second, third, and fourth years, as provided in Annex I to the proclamation.

The proclamation also excluded certain products from application of the safeguard measure. Specifically, the proclamation excluded the following:

- 10 to 60 watt, inclusive, rectangular solar panels, where the panels have the following characteristics: (A) length of 250 mm or more but not over 482 mm or width of 400 mm or more but not over 635 mm, and (B) surface area of 1000 cm<sup>2</sup> or more but not over 3,061 cm<sup>2</sup>, provided that no such panel with those characteristics shall contain an internal battery or external computer peripheral ports at the time of entry.
- 1 watt solar panels incorporated into nightlights that use rechargeable batteries and have the following dimensions: 58 mm or more but not over 64 mm by 126 mm or more but not over 140 mm.
- 2 watt solar panels incorporated into daylight dimmers that may use rechargeable batteries, such panels with the following dimensions: 75 mm or more but not over 82 mm by 139 mm or more but not over 143 mm.
- Off-grid and portable CSPV panels, whether in a foldable case or in rigid form containing a glass cover, where the panels have the following characteristics: (a) a total power output of 100 watts or less per panel; (b) a maximum surface area of 8,000 cm<sup>2</sup> per panel; (c) does not include a built-in inverter; and where the panels have glass covers, such panels must be in individual retail packaging (in this context, retail packaging typically includes graphics, the product name, its description and/or features, and foam for transport).

- 3.19 watt or less solar panels, each with length of 75 mm or more but not over 266 mm and width of 46 mm or more but not over 127 mm, with surface area of 338 cm<sup>2</sup> or less, with one black wire and one red wire (each of type 22 AWG or 24 AWG) not more than 206 mm in length when measured from panel edge, provided that no such panel shall contain an internal battery or external computer peripheral ports.
- 27.1 watt or less solar panels, each with surface area less than 3,000 cm<sup>2</sup> and coated across the entire surface with a polyurethane doming resin, the foregoing joined to a battery charging and maintaining unit, such unit which is an acrylonitrile butadiene styrene (ABS) box that incorporates a light emitting diode (LED) by coated wires that include a connector to permit the incorporation of an extension cable.

In addition to these exclusions, the proclamation directed the Trade Representative to publish a notice establishing procedures for interested persons to request the exclusion of particular products from the safeguard measure. The proclamation provided that if the Trade Representative, in consultation with the Secretaries of Commerce and Energy, determines that a particular product should be excluded, the Trade Representative can modify the HTS provisions created in Annex I of the proclamation to exclude the particular product from the safeguard measure through publication of the determination in the *Federal Register*.

On February 14, 2018, the Office of the United States Trade Representative (USTR) published a notice establishing procedures to consider requests for exclusion of particular products from the safeguard measure. The notice provided that requests for exclusion should identify the particular product in terms of the physical characteristics (e.g., dimensions, wattage, material composition, or other distinguishing characteristics)

that distinguish it from other products that are subject to the safeguard measures. USTR noted that it would not consider requests that identify the product at issue in terms of the identity of the producer, importer, or ultimate consumer; the country of origin; or trademarks or tradenames. Furthermore, USTR confirmed that it only would grant those exclusions that do not undermine the objectives of the safeguard measure.

Pursuant to that notice, USTR received 48 product exclusion requests and 213 subsequent comments responding to various requests. The types of products for which USTR received an exclusion request generally fall into seven categories: (1) products that consist of attachments or other parts that can be mounted to solar products; (2) products that constitute 72-cell or greater panels; (3) products with particular configurations for additional performance; (4) products with specialized functions; (5) consumer and specialty products; (6) bifacial panels and bifacial solar cells; and (7) solar cells without busbars or gridlines and panels containing these solar cells.

## **II. Exclusions From the Safeguard Measure**

USTR has considered certain requests for exclusion of particular products and determined that exclusion of the CSPV products described in subdivisions (c)(iii)(7) through (c)(iii)(14) of U.S. note 18 to subchapter III of chapter 99 of the HTS, as amended in the Annex to this notice, from the safeguard measure established in Proclamation 9693 would not undermine the objectives of the safeguard measure. Therefore, USTR finds that these CSPV products should be excluded from the safeguard measure. Accordingly, under the authority vested in the Trade Representative by Proclamation 9693, the Trade Representative modifies the HTS provisions created by the Annex to Proclamation 9693 as set forth in the Annex to this notice.

### **III. Past Requests Not Addressed in This Notice**

The Trade Representative has not at this time made a determination with respect to the requests for exclusion, received as of March 16, 2018, that are not addressed in the Annex to this notice. USTR will continue to evaluate those requests and the Trade Representative will make the appropriate determination in due course.

### **IV. Future Requests**

At this time, USTR is not considering additional requests for exclusion beyond those received as of March 16, 2018. USTR will monitor developments in the U.S. market for CSPV products and, if warranted, provide an opportunity to submit additional requests for exclusion at a future date.

### **V. Annex**

The following provisions supersede those currently in the HTS and are effective with respect to articles entered, or withdrawn from a warehouse for consumption, on or after 12:01 a.m., EST, on [INSERT DATE OF PUBLICATION IN THE FEDERAL REGISTER]. The HTS is modified as follows:

(1) U.S. note 18 to subchapter III of chapter 99 of the HTS is modified:

(a) By inserting the following new subdivisions in numerical sequence at the end of subdivision (c)(iii):

“(7) off-grid, 45 watt or less solar panels, each with length not exceeding 950 mm and width of 100 mm or more but not over 255 mm, with a surface area of 2,500 cm<sup>2</sup> or less, with a pressure-laminated tempered glass cover at the time of entry but not a frame, electrical cables or connectors, or an internal battery;

(8) 4 watt or less solar panels, each with a length or diameter of 70 mm or more but not over 235 mm, with a surface area not exceeding 539 cm<sup>2</sup>, and not exceeding 16 volts, provided that no such panel with these characteristics shall contain an internal battery or external computer peripheral ports at the time of entry;

(9) solar panels with a maximum rated power of equal to or less than 60 watts, having the following characteristics, provided that no such panel with those characteristics shall contain an internal battery or external computer peripheral ports at the time of entry: (A) length of not more than 482 mm and width of not more than 635 mm or (B) a total surface area not exceeding 3,061 cm<sup>2</sup>;

(10) flexible and semi-flexible off-grid solar panels designed for use with motor vehicles and boats, where the panels range in rated wattage from 10 to 120 watts, inclusive;

(11) frameless solar panels in a color other than black or blue with a total power output of 90 watts or less where the panels have a uniform surface without visible solar cells or busbars;

(12) solar cells with a maximum rated power between 3.4 and 6.7 watts, inclusive, having the following characteristics: (A) a cell surface area between 154 cm<sup>2</sup> and 260 cm<sup>2</sup>, inclusive, (B) no visible busbars or gridlines on the front of the cell, and (C) more than 100 interdigitated fingers of tin-coated solid copper adhered to the back of the cell, with the copper portion of the metal fingers having a thickness of greater than 0.01 mm;

(13) solar panels with a maximum rated power between 320 and 500 watts, inclusive, having the following characteristics: (A) length between 1,556 mm and 2,070 mm inclusive, and width between 1,014 mm and 1,075 mm, inclusive, (B) where the solar cells comprising the panel have no visible busbars or gridlines on the front of the cells,

and (C) the solar cells comprising the panel have more than 100 interdigitated fingers of tin-coated solid copper adhered to the back of the cells, with the copper portion of the metal fingers having thickness greater than 0.01 mm;

(14) modules (as defined in note 18(g) to this subchapter) incorporating only CSPV cells that are products of the United States and not incorporating any CSPV cells that are the product of any other country.”

**Jeffrey Gerrish,**

*Deputy U.S. Trade Representative.*

[FR Doc. 2018-20342 Filed: 9/18/2018 8:45 am; Publication Date: 9/19/2018]

# Robust PV Degradation Methodology and Application

Dirk C. Jordan, Chris Deline, Sarah R. Kurtz, Gregory M. Kimball, and Mike Anderson

**Abstract**—The degradation rate plays an important role in predicting and assessing the long-term energy generation of photovoltaics (PV) systems. Many methods have been proposed for extracting the degradation rate from operational data of PV systems, but most of the published approaches are susceptible to bias due to inverter clipping, module soiling, temporary outages, seasonality, and sensor degradation. In this paper, we propose a methodology for determining PV degradation leveraging available modeled clear-sky irradiance data rather than site sensor data, and a robust year-over-year rate calculation. We show the method to provide reliable degradation rate estimates even in the case of sensor drift, data shifts, and soiling. Compared with alternate methods, we demonstrate that the proposed method delivers the lowest uncertainty in degradation rate estimates for a fleet of 486 PV systems.

**Index Terms**—Degradation rates, durability, photovoltaic (PV) field performance, PV lifetime, reliability.

## I. INTRODUCTION

THE long-term performance and stability of photovoltaics (PV) modules has great impact on the economics of PV installations. Degradation rates have been summarized by Jordan *et al.* and recently updated [1]. Historically, long-term performance has been expressed as a function of initial energy generation and a longer term degradation rate, resulting in a gradual decline in annual performance. Implicit is the assumption of linear performance loss, though many PV degradation mechanisms exhibit marked nonlinearity [2]. SunPower first proposed to determine a long-term degradation rate applying a year-on-year method (YOY) [3]. Instead of a single degradation rate, a distribution of degradation rates is obtained for a single system, the median of which indicates the overall decline of the system. More recently, the YOY method was shown to have a reduced sensitivity to outliers, snow and soiling events [4].

In this paper, we introduce an additional improvement that avoids errors due to irradiance sensor drift, calibration, soiling, or misalignment. This clear-sky method can be applied

Manuscript received June 9, 2017; revised October 18, 2017; accepted November 26, 2017. This work was supported by the U.S. Department of Energy under Contract DE-AC36-08-GO28308 with the National Renewable Energy Laboratory. (Corresponding author: Dirk C. Jordan.)

D. C. Jordan, C. Deline, and S. R. Kurtz are with the National Renewable Energy Laboratory, Golden, CO 80401 USA (e-mail: dirk.jordan@nrel.gov; chris.deline@nrel.gov; Sarah.Kurtz@nrel.gov).

G. M. Kimball and M. Anderson are with the SunPower Corporation, San Jose, CA 95134 USA (e-mail: gregory.kimball@sunpower.com; michael.anderson@sunpower.com).

Color versions of one or more of the figures in this paper are available online at <http://ieeexplore.ieee.org>.

Digital Object Identifier 10.1109/JPHOTOV.2017.2779779

to any climate and is insensitive to common problems such as irradiance measurement inaccuracy. Furthermore, this technique provides a standard approach to assess the health of PV generation assets.

## II. ANALYSIS METHODOLOGY

Here we define degradation rate as a rate of change, with a negative rate representing a decrease in performance. Computing the degradation rates of PV systems from time-series data requires three primary steps which are described here: normalization, filtering, and data analysis.

### A. Normalization

This step calculates a unitless performance ratio (PR) metric with less variability than raw power production data. PR is typically based on the rated power of the system, the measured PV power, and site irradiance. In this method, we also normalize by temperature to generate a temperature-corrected PR:

$$\text{PR} = \frac{P}{P_{\text{STC,rated}} * \frac{G_{\text{POA}}}{G_{\text{ref}}} * (1 + \gamma * [T_{\text{cell}} - T_{\text{ref}}])} \quad (1)$$

where  $P$  is the measured dc or ac power of the PV system in watts,  $P_{\text{STC,rated}}$  is the rated power of the PV system in watts,  $G_{\text{POA}}$  is the plane-of-array irradiance,  $G_{\text{ref}}$  is the reference irradiance 1000 W/m<sup>2</sup>,  $\gamma$  is the maximum power temperature coefficient in relative %/°C,  $T_{\text{cell}}$  is the cell temperature in °C, and  $T_{\text{ref}}$  is the reference temperature in °C. We denote the subscript “STC” for normalization with  $T_{\text{ref}}$  of 25 °C [5] and “PTC” for normalization with  $T_{\text{ref}}$  of 45 °C [6]. Two normalization routines are compared using (1)—a conventional PR calculation ( $\text{PR}_{\text{PTC}}$ ), where  $G_{\text{POA}}$  and  $T_{\text{cell}}$  are measured with field sensors, and a clear-sky method ( $\text{PR}_{\text{CS}}$ ), where  $G_{\text{POA}}$  and  $T_{\text{cell}}$  are modeled and therefore insensitive to soiling or long-term drift.  $\text{PR}_{\text{CS}}$ , or PR relative to clear-sky conditions, requires (1) be modified as follows:

$$\text{PR}_{\text{CS}} = \frac{P}{P_{\text{STC,rated}} * \frac{G_{\text{POA,cs}}}{G_{\text{ref}}} * (1 + \gamma * [T_{\text{cell,cs}} - T_{\text{ref}}])} \quad (2)$$

where  $G_{\text{POA,cs}}$  is the modeled clear-sky plane-of-array irradiance and  $T_{\text{cell,cs}}$  is the modeled clear-sky cell temperature.  $\text{PR}_{\text{CS}}$  uses a static model of expected power that does not change from one year to the next. Since this model does not account for weather or cloud effects, only clear-sky conditions can be included in the subsequent degradation rate calculation.

The model of clear-sky irradiance was based on PV system configuration data and modeling tools publicly available in PVLIB [7]. The site details required are longitude, latitude, time zone, altitude, and PV system mounting configuration. The ground albedo was assumed to be 20% for all systems in the study. Using atmospheric turbidity derived from Linke turbidity parameters, the Ineichen irradiance model generates global horizontal, direct normal and diffuse horizontal irradiance values [8]. The horizontal irradiance is then transposed to the array plane using PVLIB's King transposition model [7].

The model of clear-sky temperature was based on site location as well as monthly average daytime and nighttime temperatures. Temperature data were obtained in high-resolution image format from NASA Earth Observatory with 0.05° spatial resolution [9]. The source data consisted of monthly long-term average day and night temperatures, which were then interpolated to 15-min data using mean values of a rolling 20-day Gaussian window. The following equation computed the clear-sky ambient temperature:

$$T_{\text{amb,cs}} = \frac{(T_{\text{day}} - T_{\text{night}})}{2} * \cos\left(\frac{h + 8.0}{24} * 2\pi\right) + \frac{(T_{\text{day}} + T_{\text{night}})}{2} \quad (3)$$

where  $T_{\text{day}}$  is the average monthly day temperature in °C,  $T_{\text{night}}$  is the average monthly night temperature in °C, and  $h$  is the time since midnight in hours. The factor 8 in the cosine term is an empirical factor taking into account the lag between daily peak irradiance and temperature. Clear-sky cell temperature for an assumed polymer backsheet and rack-mounted PV system was then derived from the field validation work of King *et al.* using the following relation [10]:

$$T_{\text{cell,cs}} = T_{\text{amb,cs}} + G_{\text{poa,cs}} * e^{-3.56} + \frac{G_{\text{poa,cs}}}{333}. \quad (4)$$

The parameter gamma ( $\gamma$ ) in (1) and (2) is used to capture the differences in thermal behavior between wafer and thin film PV cell materials, and is extracted from the PV module datasheets. Although we expect differences in (4) as a function of PV system mounting and module construction, the precision of the temperature model contributes less uncertainty than the use of long-term average ambient temperature data in place of temperature sensors.

### B. Filtering

The filtering step removes data collected during periods of poor or variable solar resource conditions as well as nonrepresentative or biasing data. First, low irradiance conditions are often associated with nighttime data or with errors due to inverter startup and nonuniform irradiance (see Fig. 1). We have found a low irradiance cutoff of 200 W/m<sup>2</sup> to exclude these start-up issues without removing winter data from high latitude locations. Second, a clear-sky index (csi) filter is used, where csi is the ratio of measured irradiance to modeled clear-sky irradiance. Fig. 1(b) indicates the impact of a window filter of variable width (e.g., +/- 10%) around csi equals to 1. We have evaluated csi filters of width 10% and 20% in this analysis. Third,

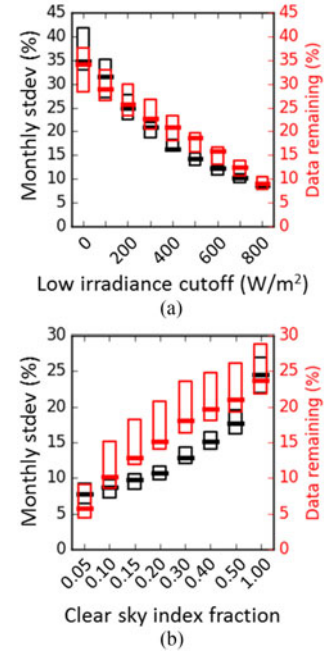


Fig. 1. Monthly standard deviation in  $PR_{CS}$  (left axis) and remaining data (right axis) for ranges of (a) low irradiance cut-off and (b) clear-sky index fraction values.

systems with high dc/ac ratio can be limited during normally high producing days by the input window of the inverter possibly biasing long-term performance assessment. Therefore, we filtered out periods of inverter clipping by excluding data during which power was >99% of the maximum value. Machine-learning algorithms to automatically detect inverter clipping may be useful and incorporated in future work. Finally, an operational filter excluded data outside of a  $\pm 30\%$  band around a 3-month rolling median performance index to identify the rare case where systems are offline for maintenance.

### C. Analysis

The analysis step processes the remaining data to compute a degradation rate based on one of the three methods. In the YOY method, the rate of change is calculated between two points at the same time in subsequent years. Calculating such a rate of change for all data points and all years, results in a histogram of rates of change, the central tendency of which representing the overall system performance. Further details on the methodology can be found in [3] or [4]. In contrast, the standard least square regression (SLS) approach uses all data points in a single regression by minimization of the difference between the model and the data. Finally, the quantile regression is a form of robust regression using quantiles instead of the response mean. [11] Prior to degradation analysis, the normalized, filtered 15-min data are aggregated over a variable time period. Fig. 2(a) shows a decreasing standard deviation of YOY deltas with the number of aggregation days. In general, since long aggregation periods reduce the number of points considered per regression, we found that a 7-day aggregation period delivered satisfactory results. Therefore, unless otherwise stated, 7-day aggregation levels were used in the remainder of the paper.

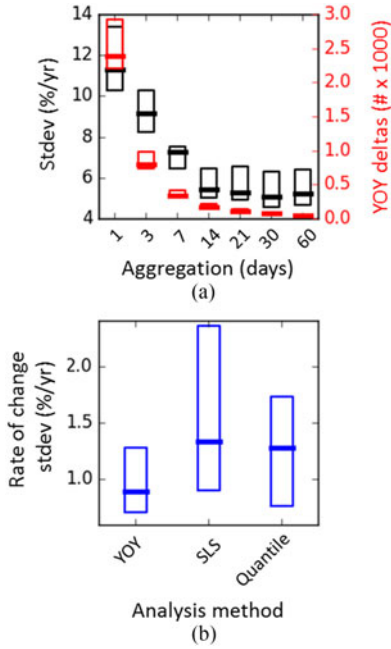


Fig. 2. (a) For the YOY method, increasing the aggregation window results in lower standard deviation in the distribution of year-on-year deltas. (b) The YOY method shows the lowest standard deviation in degradation rates compared with SLS and quantile regression when an inverter is repeatedly analyzed each month.

Fig. 2(b) shows results of the three analysis approaches (YOY, SLS, quantile regression) for the fleet of systems considered in Section IV-B. The YOY method shows the lowest standard deviation in degradation rates compared with SLS and quantile regression, suggesting that the YOY method can yield more consistent degradation estimates.

An example comparison between the two YOY normalization methods is shown for an x-Si PV system at NREL in Fig. 3. The  $PR_{PTC}$  using a calibrated pyranometer is overlaid with the  $PR_{CS}$ . For PV systems with well-maintained pyranometers, both  $PR_{PTC}$  and  $PR_{CS}$  result in approximately the same degradation rate estimate; however, the  $PR_{CS}$  has a higher uncertainty and seasonality for a variety of reasons such as errors in modeled temperature and irradiance and snow on the modules. The analytical method outlined above is also publicly available in “Rd-tools” allowing customization of the above-listed assumptions. [12] For example, the albedo assumption may lead to deviation between the modeled and the measured clear-sky irradiance. As long as the irradiance model is approximately modeling clear conditions within this range, we recommend a clear sky index threshold between 10% and 20% to appropriately exclude cloudy, variable irradiance conditions but to allow for potential drift of irradiance sensors.

### III. COMMON EVALUATION QUANDARIES

PV systems with verified irradiance sensor calibration and maintenance are most desirable for long-term performance evaluation, and resulted in a cleaner dataset in Fig. 3. Unfortunately, these conditions are not always met in real-world systems.

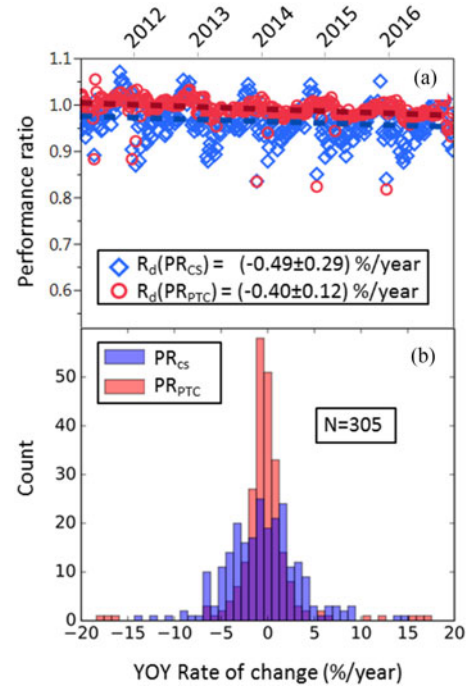


Fig. 3. (a) Performance ratio of a single system at NREL using  $PR_{PTC}$  and  $PR_{CS}$  as a function of time with respective SLS regression lines. (b) Year-on-year aggregated histograms for the respective PR’s. The rate of change values noted in (a) are taken as the medians of the two histograms shown in (b). In addition, the number of data points in the histograms is also given.

#### A. Drifting Irradiance Sensor

The most critical yet often unknown variable is the calibration state of the irradiance sensor. We performed the  $PR_{CS}$  methodology from Section II on the same PV system using different sources of  $G_{poa}$  data. Fig. 4(a) shows the ratio of various  $G_{poa}$  sensors with respect to a regularly calibrated system pyranometer. As a guide to the eye, a no-change line at unity is given by a solid line. The median of ten independently calibrated yet different pyranometers and reference cell one at NREL show flat behavior with respect to the calibrated system pyranometer, indicating no long-term drift within the measurement uncertainty. In contrast, two uncalibrated photodiodes and a second reference cell show marked drift over 5 years at an annualized linear rate of 1%–2%/year, although some sensors drift appears nonlinear.

Fig. 4(b) displays the results using the different sensor and using the  $PR_{PTC}$  and  $PR_{CS}$  metrics. The green bands indicate the  $1\sigma$  standard deviation or 68% confidence interval from a more conventional analysis of ten different methods [13] that include various time-series analyses and independent quarterly  $I-V$  measurements. When the calibrated sensors are used, the degradation rates generally fall into the green band of expected degradation regardless of the PR metric. In contrast, serious deviations can be discerned for the drifting sensors. Using  $PR_{PTC}$  with a drifting  $G_{poa}$  sensor results in grossly incorrect performance assessment, but using  $PR_{CS}$  results in degradation assessment close to the expected range. When using the  $PR_{CS}$  metric, applying a  $\pm 20\%$  csi filter results in degradation rates within the expected range, but applying a  $\pm 10\%$  csi filter

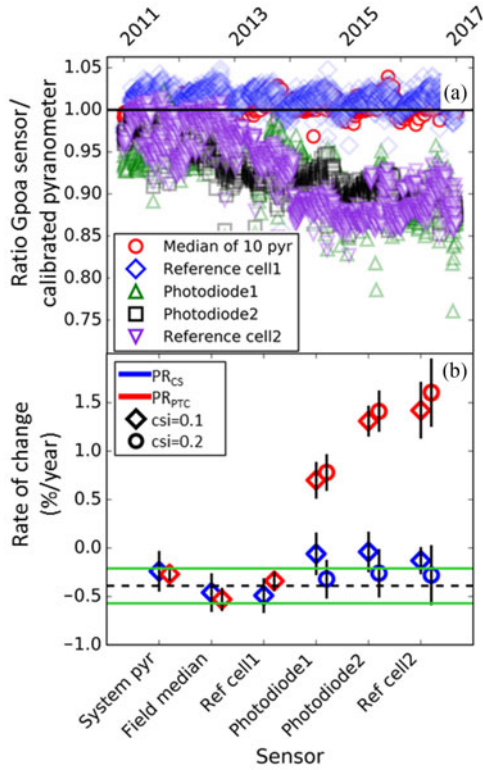


Fig. 4. (a) Ratio of various  $G_{poa}$  sensors with respect to a calibrated reference  $G_{poa}$  pyranometer. Shown are the median of ten pyranometers in the same yard at NREL, two reference cells, and two photodiodes. As guide to the eye, a no-change line is given by a solid line. (b) Rate of change determined using the various  $G_{poa}$  sensors on the same system of Fig. 3(b). The red markers use the respective  $G_{poa}$  sensor while the blue markers use the clear-sky method. The green interval is the band of degradation for this system (see text) and two different csi filters are indicated by different symbols.

results in degradation rates somewhat outside the expected range. In this example, the  $\pm 10\%$  csi filter removes too much data for the heavily degraded sensor and adds positive bias. In the case of severe sensor degradation even as high as  $>1.5\%/yr$ , the PR<sub>CS</sub> metric allows for accurate assessment of the degradation rate.

### B. Data Shifts

Data shifts are often induced unintentionally in practice by the replacement of hardware or changes in software configuration. For example, the large shift displayed in Fig. 5(a) was caused by the replacement of a dc power sensor. Fig. 6 compares the degradation rate using three different techniques for handling data shifts. The technique of “shift correction” adjusts the data based on the minimization of the root mean square error from a regression. [14] However, this requires knowledge of the degradation curve that is commonly assumed to be linear, but may take on a variety of shapes. The technique of “Removal” uses the YOY approach to highlight and exclude a secondary peak, see Fig. 5(b), caused by the data shift. The technique of “two step” evaluates the data in two steps by separating the sections before and after the shift and then aggregating the YOY deltas into a combined histogram. The SLS regression for the two-step procedure is combined by evaluating the median of the

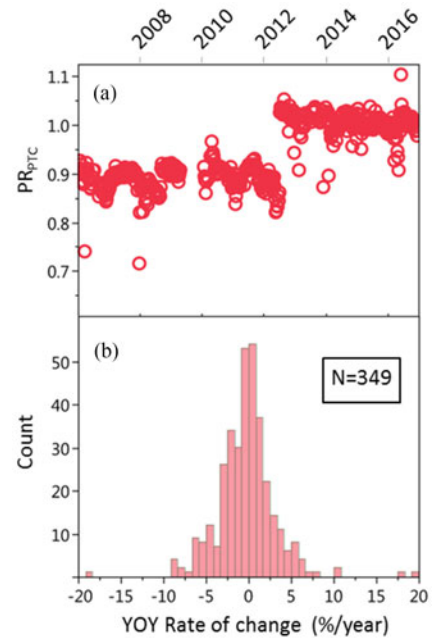


Fig. 5. (a) Data shift occurrence because of a maintenance event of the dc measurement sensor. (b) Resulting secondary peak in the PR<sub>PTC</sub> year-on-year histogram.

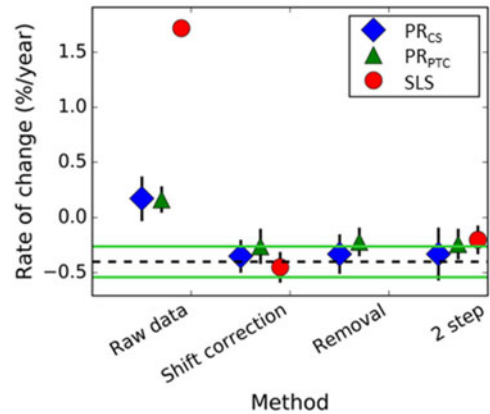


Fig. 6. YOY PRs and SLS for different data shift correction procedures compared with evaluation with the uncorrected data. The green interval is the band of degradation for this system based primarily on ten more conventional time series analyses and independent tests such as  $I-V$  measurements.

two separate degradation rates combined with a pooled standard deviation. Fig. 6 compares the degradation rate using three different data shift correction techniques. The green interval is a band of degradation determined similarly to Section III-A. Because the interval relies mostly on shift correction and regression approaches, the interval should be viewed as an approximate guideline rather than an accurate confidence interval of the system performance. The greatest sensitivity to the data shift of the uncorrected data is shown by the SLS. Although the YOY approaches are biased by the data shift, the sensitivity is far less compared with SLS. Because the removal method requires the application of the YOY method, the SLS is not applicable and therefore absent from the “Removal” dataset in Fig. 6. Within the uncertainty, the data shift correction methods appear to be

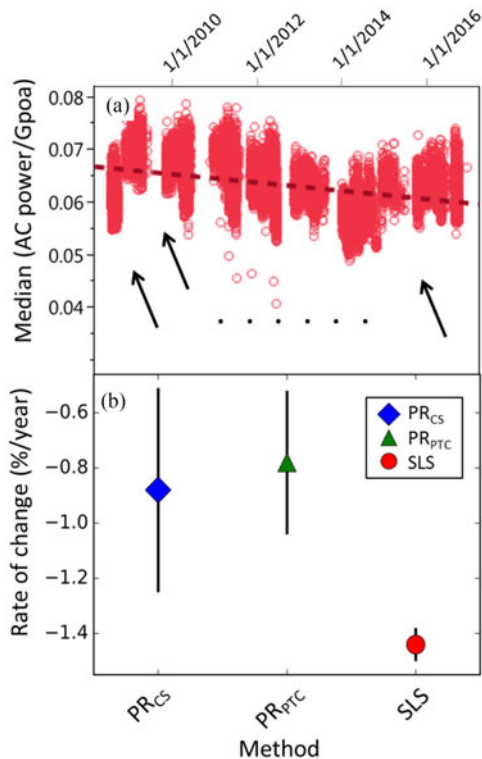


Fig. 7. (a) PV system in southern California exhibiting substantial seasonal soiling intervals some marked by arrows. (b) Results of the YOY approach compared with a SLS regression approach.

approximately equivalent for the performance metrics although the YOY methods appear perhaps slightly more consistent. In reality, most data shifts are not as pronounced and easily detectable as in this example, in which case the sensitivity of the SLS regression can be of considerable concern.

### C. Soiling

Soiling has seen an increased interest in recent years because of its significant impact on the project economics in some locations. Fig. 7 shows the ac power from a PV system in southern California that exhibits considerable soiling intervals, some of which are indicated by arrows. Reversible performance changes can introduce bias into degradation analysis. Linear methods such as SLS regression or quantile regression are particularly sensitive to bias resulting from anomalous performance at the beginning or end of the evaluation period, which is known in statistics as high leverage. In addition, SLS methods are sensitive to bias due to the largest reversible fluctuations caused by soiling.

To obtain an unbiased performance assessment with linear methods, the soiling events would have to be carefully removed from time-series data requiring detailed knowledge from a soiling station, where one module, for example, is permitted to natural soil, while another one is cleaned on a regular basis. Fig. 7 highlights the importance of using YOY methods instead of linear regression to analyze time-series data that has been affected by soiling. Applying the YOY approach for both PR methods reduces error associated with soiling, see Fig. 7(b),

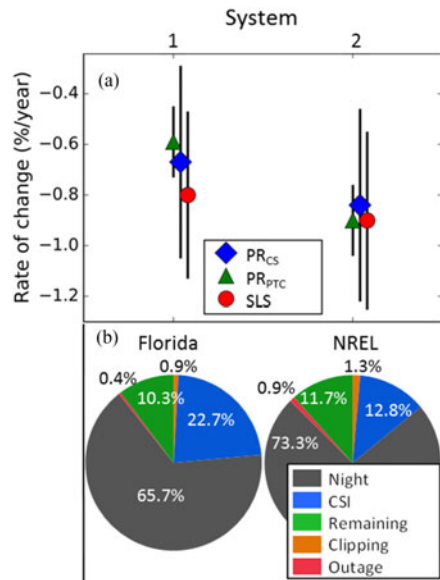


Fig. 8. (a) Two PV systems located near Pensacola, Florida that showed more partly cloudy days. (b) Data percentage impact of the described filters for the Florida systems and a comparable system at NREL.

especially seasonally occurring soiling trends, as shown before [4].

### D. Cloudy Climates

With the emphasis on clear-sky conditions, it is important to demonstrate how the proposed method performs in locations where cloudy conditions occur more often. Significant installed PV capacity and frequent partly cloudy conditions in Florida make this an excellent region for demonstrating the effectiveness of the methods in lower irradiance climates, as displayed in the inset of Fig. 8(a). We applied the proposed method to two systems on a school building near Pensacola, FL, that some of the authors evaluated in 2012. Fig. 8(a) shows that the proposed method resulted in very good agreement with the more traditional time-series approach of the earlier evaluation [15]. In addition, we provide the data percentage impact of the described filters for the systems in Florida in comparison with a similar system at NREL during the same 4.5 years of operation. None of the systems experienced major operational outages or significant inverter clipping. It should be noted that these pie charts may differ depending on location, design, operational consistency, and data quality. The majority of the data is removed due to low irradiance or night time filter. The number of remaining data points and the impact of the outage and clipping filter are approximately the same for both systems. Even with the cloudier conditions leading to greater csi filtering, the Florida system still had sufficient remaining data to enable successful analysis. However, longer evaluation periods may be required as the cloudiness increases.

### E. Nonlinearities

The implicit assumption in the analysis above is the linearity of the long-term degradation curve. However, PV degradation

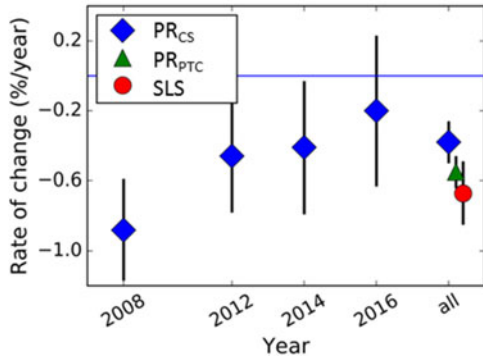


Fig. 9. Nonlinear trend for a heterojunction crystalline silicon (x-Si) system using the  $PR_{CS}$  metric. The time series is evaluated in 2 year increments along with cumulative total degradation rates using multiple performance metrics.

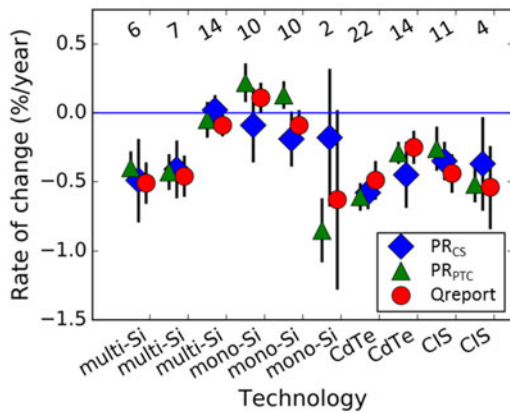


Fig. 10. Comparison of the various systems at NREL using the year-on-year approach using  $PR_{CS}$  and  $PR_{PTC}$  contrasted to a quarterly report (Qreport) that consists of ten more conventional time-series analysis and independent tests such as  $I-V$  measurements. The number above each system indicates the systems' age in years.

may not be linear over the life of the system. Depending on the underlying degradation mechanisms, the degradation curve of a PV system may exhibit substantial deviation from linearity [2]. In the case of suspected nonlinearity, the entire datasets can be divided into shorter sections, as illustrated in Fig. 9. This system, which was installed at the end of 2007, exhibited a higher degradation in the first 2 years than in subsequent years using  $PR_{CS}$ , which was aggregated in 7 days [16]. Because of field upgrades, during which time the system was not field exposed, a gap on the time axis is present. In addition, the degradation rates for the entire dataset using different performance metrics are also displayed. Even as the uncertainties for the 3 metrics overlap, the YOY methods show a degradation rate that is closer to the year 3–9 behavior than the SLS regression.

#### IV. APPLICATIONS

##### A. Validation With NREL PV Systems

NREL maintains an array of PV systems representing many PV module technologies and an operating history  $>10$  years. In addition to continuous monitoring, the PV systems are characterized by periodic  $I-V$  curve measurements, infrared imaging, and visual inspection. NREL prepares quarterly reports on the

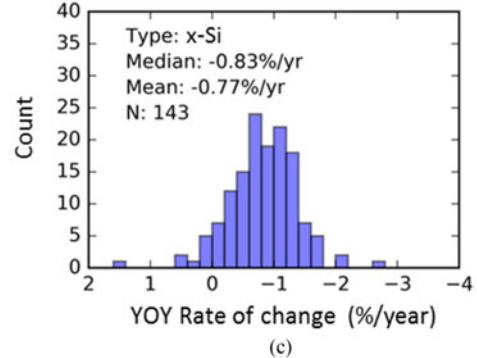
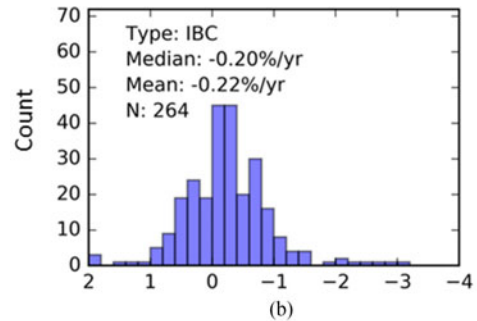
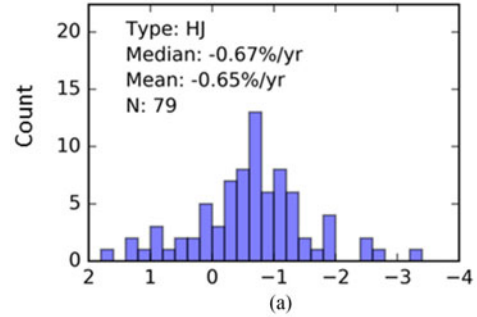


Fig. 11. Aggregated degradation rates derived from the  $PR_{CS}$  YOY method for a fleet of systems partitioned by technology, (a) heterojunction, (b) interdigitated backcontact, (c) and all other x-Si.

performance of each PV system based on time-series analysis using a variety of methods. The results of the most recent report were compared with the results of a new study based on  $PR_{CS}$  and  $PR_{PTC}$  normalization and YOY analysis. Fig. 10 shows good agreement between the methods used in the quarterly report and the methods outlined in Section II.

##### B. PV Fleet Roll-Up

The  $PR_{CS}$  clear-sky method described in Section II was applied to PV electricity-production data from a group of 486 inverters to demonstrate the wide applicability of the method. The analysis was performed by SunPower using software tools shared between NREL and SunPower. The PV systems were commissioned between 2006 and 2011, with a mean operating age of 7.3 years and total STC capacity of 230 MW. The data represent one of the largest sets of PV system time-series analysis in the literature, and the minimum age of 6 years reduces the impact of LID and other short-term stabilization effects. The data presented in [17] overlap in part with the data presented in Fig. 11, with a critical difference that in this paper clear sky

models of sensor values are used instead of raw measured sensor data for normalizing PV power. As PV systems age, they are more likely to accumulate outages or degradation in irradiance or temperature sensors, so the methods presented in Section II are expected to grow in importance as time-series data on older systems become available. Degradation analysis was performed for each PV system, and statistics were computed for the population of PV systems based on the module technology (see Fig 11). The median degradation rate for PV systems with heterojunction (HJ) modules is similar to a more detailed HJ system investigation by Jordan *et al.*[16], while the fleet of interdigitated back contact (IBC) modules showed a statistically significant lower rate of change than the HJ and the fleet of other crystalline silicon (x-Si) systems. Distilling further statistically significant trends was difficult because of the convolution of the time series, technology, temperature, and mounting differences and awaits further investigation.

## V. CONCLUSION

We present a robust methodology for estimating the degradation rate of PV systems by combining the YOY method with clear-sky modeling. The clear-sky normalization step prevents bias due to poor maintenance or irregular calibration of irradiance and temperature sensors. The filtering approach mitigates bias due to inverter clipping and temporary outages as well as noise due to nonuniform irradiance. The YOY analysis limits the impact of data shifts, soiling, and nonlinearity as compared with linear methods. When analyzing high-quality data from PV systems at NREL, the proposed methodology yielded similar degradation rate estimates to those published previously. Applying the robust methodology to a fleet of PV systems, we were able to discriminate between the long-term degradation behavior of different technologies including HJ and IBC.

## ACKNOWLEDGMENT

The authors would like to thank A. Shinn, A. Nag, M. Deceglie, B. Bourne, K. Davis, NREL's reliability and measurement group.

## REFERENCES

- [1] D. C. Jordan, S. R. Kurtz, K. T. VanSant, and J. Newmiller, "Compendium of photovoltaic degradation rates," *Prog. Photovolt. Res. Appl.*, vol. 24, no. 7, pp. 978–989, 2016, doi:[10.1002/pip.2744](https://doi.org/10.1002/pip.2744).
- [2] D. C. Jordan, T. J. Silverman, B. Sekulic, and S. R. Kurtz, "PV degradation curves: Non-linearities and failure modes," *Prog. Photovolt. Res. Appl.*, vol. 25, pp. 583–591, 2016, doi:[10.1002/pip.2835](https://doi.org/10.1002/pip.2835).
- [3] E. Hasselbrink *et al.*, "Validation of the PVLife model using 3 million module-years of live site data," in *Proc. 39th IEEE Photovolt. Spec. Conf.*, Tampa, FL, USA, 2013, pp. 7–13, doi:[10.1109/PVSC.2013.6744087](https://doi.org/10.1109/PVSC.2013.6744087).
- [4] D. C. Jordan, M. G. Deceglie, and S. R. Kurtz, "PV degradation methodology comparison — A basis for a standard," in *Proc. 43rd IEEE Photovolt. Spec. Conf.*, Portland, OR, USA, 2016, pp. 0273–0278, doi:[10.1109/PVSC.2016.7749593](https://doi.org/10.1109/PVSC.2016.7749593).
- [5] STC: Irradiance = 1000 W/m<sup>2</sup>, Air mass = 1.5, Module temperature = 25 °C.
- [6] T. Dierauf, A. Growitz, S. Kurtz, J. L. Becerra Cruz, E. Riley, and C. Hansen, "Weather-corrected performance ratio," Nat. Renewable Energy Lab., Golden, CO, USA, Tech. Rep. NREL/TP-5200-57991, Apr. 2013.
- [7] J. S. Stein, W. F. Holmgren, J. Forbess, and C. W. Hansen, "PVLIB: Open source photovoltaic performance modeling functions for Matlab and Python," in *Proc. 43rd IEEE Photovolt. Spec. Conf.*, Portland, OR, USA, 2016, pp. 3425–3430.
- [8] P. Ineichen and R. Perez, "A New airmass independent formulation for the Linke turbidity coefficient," *Sol. Energy*, vol. 73, pp. 151–157, 2002.
- [9] [Online]. Available: [https://neo.sci.gsfc.nasa.gov/view.php?datasetId=MOD\\_LSTD\\_CLIM\\_M](https://neo.sci.gsfc.nasa.gov/view.php?datasetId=MOD_LSTD_CLIM_M)
- [10] D. L. King, J. A. Kratochvil, and W. E. Boyson, *Photovoltaic Array Performance Model*. Albuquerque, NM, USA: Sandia Nat. Lab., Aug. 2004.
- [11] R. Koenker and G. J. Bassett, "Regression quantiles," *Econometrica*, vol. 46, no. 1, pp. 33–50, 1978.
- [12] 2017. [Online]. Available: <https://github.com/NREL/rdtools>
- [13] D. C. Jordan and S. R. Kurtz, "Thin-film reliability trends toward improved stability," in *Proc. 37th IEEE Photovolt. Spec. Conf.*, Seattle, WA, USA, 2011, pp. 000827–000832, doi:[10.1109/PVSC.2011.6186081](https://doi.org/10.1109/PVSC.2011.6186081).
- [14] D. C. Jordan and S. R. Kurtz, "Analytical improvements in PV degradation rate determination," in *Proc. 35th IEEE Photovolt. Spec. Conf.*, Honolulu, HI, USA, 2010, pp. 002688–002693.
- [15] K. O. Davis, S. R. Kurtz, D. C. Jordan, J. H. Wohlgemuth, and N. Sorloaica-Hickman, "Multi-pronged analysis of degradation rates of photovoltaic modules and arrays deployed in Florida," *Prog. Photovolt. Res. Appl.*, vol. 21, pp. 702–712, 2012.
- [16] D. C. Jordan *et al.*, "Silicon heterostructure PV system field performance," in *Proc. 44th IEEE Photovolt. Spec. Conf.*, Washington DC, USA, 2017, pp. 1–6.
- [17] A. J. Curran *et al.*, "Determining the power rate of change of 353 plant inverters time-series data across multiple climate zones, using a month-by-month data science analysis," in *Proc. 44th IEEE Photovolt. Spec. Conf.*, Washington, DC, USA, 2017.

Authors' photographs and biographies not available at the time of publication.